

UCLA

UCLA Previously Published Works

Title

Hippocampal subregions and networks linked with antidepressant response to electroconvulsive therapy

Permalink

<https://escholarship.org/uc/item/48k5r5vc>

Journal

Molecular Psychiatry, 26(8)

ISSN

1359-4184

Authors

Leaver, Amber M
Vasavada, Megha
Kubicki, Antoni
[et al.](#)

Publication Date

2021-08-01

DOI

10.1038/s41380-020-0666-z

Peer reviewed



Hippocampal subregions and networks linked with antidepressant response to electroconvulsive therapy

Amber M. Leaver, PhD^{1,3,*}, Megha Vasavada, PhD¹, Antoni Kubicki, BS¹, Benjamin Wade, PhD¹, Joana Loureiro, PhD¹, Gerhard Hellemann, PhD², Shantanu H. Joshi, PhD¹, Roger P. Woods, MD^{1,2}, Randall Espinoza, MD MPH², Katherine L. Narr, PhD^{1,2}

¹Ahmanson-Lovelace Brain Mapping Center, Department of Neurology, University of California Los Angeles, Los Angeles, CA, 90095

²Department of Psychiatry and Biobehavioral Sciences, University of California Los Angeles, Los Angeles, CA, 90095

³Center for Translational Imaging, Department of Radiology, Northwestern University, Chicago, IL, 60611

Abstract

Electroconvulsive therapy (ECT) has been repeatedly linked to hippocampal plasticity. However, it remains unclear what role hippocampal plasticity plays in the antidepressant response to ECT. This magnetic resonance imaging (MRI) study tracks changes in separate hippocampal subregions and hippocampal networks in patients with depression (n=44, 23 female) to determine their relationship, if any, with improvement after ECT. Voxelwise analyses were restricted to the hippocampus, amygdala, and parahippocampal cortex, and applied separately for responders and nonresponders to ECT. In analyses of arterial spin-labeled (ASL) MRI, nonresponders exhibited increased cerebral blood flow (CBF) in bilateral anterior hippocampus, while responders showed CBF increases in right middle and left posterior hippocampus. In analyses of gray-matter volume (GMV) using T1-weighted MRI, GMV increased throughout bilateral hippocampus and surrounding tissue in nonresponders, while responders showed increased GMV in right anterior hippocampus only. Using CBF loci as seed regions, BOLD-fMRI data from healthy controls (n=36, 19 female) identified spatially separable neurofunctional networks comprised of different brain regions. In graph theory analyses of these networks, functional connectivity within a hippocampus-thalamus-striatum network decreased only in responders after two treatments and after index. In sum, our results suggest that the location of ECT-related plasticity within the hippocampus may differ according to antidepressant outcome, and that larger amounts of hippocampal plasticity may not be conducive to positive antidepressant response. More focused targeting of hippocampal subregions and/or circuits may be a way to improve ECT outcome.

Users may view, print, copy, and download text and data-mine the content in such documents, for the purposes of academic research, subject always to the full Conditions of use:http://www.nature.com/authors/editorial_policies/license.html#terms

*Corresponding Author: Amber M. Leaver Ph.D., Address: 737 N Michigan Ave, Suite 1600, Chicago, IL 60611, Phone 312 694 2966, Fax 310 926 5991, amber.leaver@northwestern.edu.

CONFLICT OF INTEREST

All authors declare no conflicts of interest.

INTRODUCTION

Electroconvulsive therapy (ECT) is an effective treatment for severe treatment-refractory depression, yet a mechanistic understanding of this intervention remains elusive. The most consistently reported site of ECT-related neuroplasticity is the hippocampus. This includes increases in a variety of neuroimaging markers of gray matter in humans (1–5), increased cellular plasticity including neurogenesis in animal models (6–8), and several reports of associated neurofunctional plasticity (9–12).

However, the nature of the link between hippocampal plasticity and antidepressant response to ECT is unclear. The majority of previous human structural neuroimaging studies have reported no correlation between improved depressive symptoms and gray-matter changes in hippocampus and/or surrounding cortical tissue (2–4, 13–15). In a recent report, we demonstrated that resting brain activity increased in the right anterior hippocampus after ECT, measured with arterial-spin labelled (ASL) fMRI. However, this hippocampal plasticity appeared to be more pronounced in nonresponders, suggesting that robust regional plasticity within the hippocampus may be detrimental to successful outcome (16), consistent with a recent mega-analysis of structural MRI data (15). Notably, in white-matter connections linked to this right anterior hippocampal region, microstructural markers changed after ECT in responders but not nonresponders in another of our recent studies (17). Taken together, existing literature paints a complex picture of the potential relationships between regional and network plasticity within the hippocampus with regard to antidepressant response to ECT.

The hippocampus is topographically and functionally organized, with afferent and efferent connections with the remainder of the brain varying along its anterior-posterior axis (18, 19). Thus, perhaps the precise location(s) of plasticity within the hippocampus determines which “down-stream” brain networks and regions outside the hippocampal complex are affected by ECT-related seizure activity and/or associate with clinical response. Furthermore, these patterns of plasticity may in turn impact antidepressant outcome and side effects. We attempt to address this hypothesis in this paper.

The goal of this study was to understand the relationship between antidepressant response to ECT and functional and structural change in hippocampal regions and networks. First, we measured loci of CBF (ASL-fMRI) and GMV (sMRI) change in the medial temporal lobe in patients with treatment-refractory depression undergoing ECT. Patients were grouped according to antidepressant outcome, and we attempted to identify separable loci of CBF and GMV change in responders and nonresponders to ECT (i.e., >50% or <50% improvement in depression scores, respectively). Then, we sought to determine whether these different sites of CBF change were connected with different hippocampal networks measured with BOLD-fMRI using data from non-depressed controls. Finally, we measured plasticity within these networks according to ECT response with graph theory analyses. Potential associations between all MRI metrics and recall memory were also explored. Taken together, these analyses tested the hypothesis that the location of ECT-related plasticity within the hippocampus associates with ECT outcome, which then relates to differences in network-level functional change throughout the brain.

MATERIALS AND METHODS

Subjects

Patients with treatment-refractory depression (n=57) and demographically similar non-depressed volunteers (n=36) gave informed written consent to participate in this UCLA IRB-approved study (inclusion/exclusion criteria in Supplemental Methods). Clinical response was defined as a 50% reduction in mean composite score across three depression inventories (Supplemental Methods). Prior publications overlapping with the current cohort reported ECT-related structural (17, 20–23), functional (10, 24, 25), and neurochemical (12, 26) changes, and evaluation of cognitive measures (27).

Study Visits

Patients volunteered for this research study before initiating a clinically prescribed course of ECT at the UCLA Resnick Neuropsychiatric Hospital administered using standard protocols (Supplemental Methods). Patients completed four visits: 1) within 24 hours before first ECT session (baseline), 2) immediately before their third ECT appointment (~4 days after baseline), 3) after their clinically determined ECT index series (~4 weeks after baseline), and 4) approximately 6 months after ECT index. Non-depressed volunteers completed two study visits approximately 4 weeks apart.

At each visit, volunteers underwent multimodal MRI, cognitive testing, and depression inventories. Cognitive tests are described for this cohort elsewhere (27); here, we targeted delayed recall memory of visuospatial (Brief Visuo-Spatial Memory Test Revised, BVMT) and verbal stimuli (Hopkins Verbal Learning Test Revised, HVLT), due to previously established links between the hippocampus and recall memory (28, 29).

Image Acquisition & Preprocessing

A 3T Siemens Allegra scanner acquired all images; sequence parameters are described in Supplemental Methods.

During ASL preprocessing, images were first corrected for motion (FSL; *FMRIB, Functional MRI of the Brain*), and CBF was quantified using simple subtraction in ASLtoolbox (30). Quantified images were averaged to yield a single CBF image per session for subsequent analysis. Upon visual inspection, 7 baseline (3 patients, 4 controls) and 13 follow-up (10 patients, 3 controls) ASL scans were identified to have poor quality (i.e., susceptibility artifacts, slice artifacts, and/or global CBF <20 mL/100g/min) and were not analyzed further. Global CBF was calculated for each ASL-CBF image by averaging voxelwise CBF within a gray-matter mask (SPM8 GM template >20%, ASL pseudo-BOLD >100 (30)).

Voxelwise gray matter volume (GMV) was calculated in SPM8 using the Segmentation procedure embedded with standard MNI normalization of T1-weighted structural images (31). In brief, images were corrected for intensity bias and segmented by tissue type using prior probability maps (International Consortium for Brain Mapping). Grey matter images were then modulated to reflect the degree of local deformation during spatial normalization

to produce voxelwise GMV metrics (i.e., voxel based morphometry). All GMV images passed visual inspection for quality.

BOLD images were preprocessed using FSL, including slice-time correction, motion correction, and high-pass filter (0.01 Hz). Two leading functional volumes were discarded prior to preprocessing. ICA-based denoising was also applied as described previously (25). All BOLD images passed inspection for quality.

Preprocessed ASL and BOLD images were aligned to each subject's MPRAGE using FSL, and all images (ASL, BOLD, GMV) were MNI-normalized using a nonlinear transformation and interpolated to $2 \times 2 \times 2 \text{ mm}^3$ resolution in SPM8. Spatial smoothing was applied in FSL using a 6mm FWHM Gaussian kernel.

Voxelwise Statistical Analyses

All statistical analyses were completed in R (<https://www.r-project.org>). Voxelwise statistical analyses were limited to an anatomical mask of the hippocampus, amygdala, and parahippocampal gyrus (Harvard-Oxford Atlas in FSL).

To address the *a priori* hypothesis that the location of peak CBF and GMV change differed in responders and nonresponders to ECT, CBF and GMV images from responders and nonresponders were analyzed separately using linear-mixed effects models. To identify locations of CBF change, time was the fixed factor of interest (baseline vs. post-index) and nuisance variables included age, ECT electrode placement (% right-unilateral), total number of treatments, voxelwise gray matter volume, (fixed factors) and subject (random factor). To identify locations of GMV change, time was the fixed effect of interest (baseline vs. post-index), and nuisance regressors included age, ECT electrode placement (% right-unilateral), total number of treatments, (fixed) and subject (random). For completeness, these same models were applied to the entire sample to identify main effects of time in all patients (with mean % change in depression scores as an additional fixed nuisance factor), and interactions between time and response (mean % depression score change).

The location of peak CBF and GMV change was identified separately in responders and nonresponders using an initial exploratory threshold of $p < 0.05$ $k > 25$ and validated using leave-one-out subsampling requiring 100% overlap at $p < 0.05$ across all subsample tests in each group ($k > 25$; Supplemental Methods). Clusters of CBF and GMV change were retained that met threshold $p < 0.05$ across 100% of subsample tests in each group ($k > 25$). Cluster locations consistent across 100% of subsample tests were considered robust (i.e., not due to Type I error); this assumption was tested using subsampling in control data (Supplemental Methods). Validated CBF clusters were used as seed regions for subsequent network analyses. Conventional correction methods addressing Type 1 error are also reported in figures (i.e., FDR-corrected $q < 0.05$ for voxels and RFT-corrected $p < 0.05$ for clusters).

In all regions of CBF and GMV change after ECT identified for responders and nonresponders, post-hoc region-of-interest (ROI) analyses explored interactions between time and response (% depression score change) using linear mixed models as described

above, with FDR-correction within each MRI metric (i.e., separately for CBF and GMV). Main effects of time were also explored in each group (responders, nonresponders, all patients, and controls).

Network Analyses

BOLD-fMRI data from non-depressed controls were used to define hippocampal networks (Supplemental Methods) using CBF clusters validated using subsampling procedures. Subsequent graph theory analyses using BOLD-fMRI data in depressed patients measured whether connectivity within these hippocampal networks changed after ECT, separately in responders and nonresponders (Supplemental Methods). Overall network strength and hippocampal centrality were derived for each hippocampal network and each dataset (i.e., each patient's MRI session). Linear mixed effects models examined interactions between time and response (% depression score change) for both acute (after 2 treatments) and post-treatment (after index) changes, where nuisance variables included age, ECT electrode placement (% right-unilateral), total number of treatments, (fixed factors) and subject (random factor). Statistics were FDR-corrected within each network metric (i.e., separately for network strength and hippocampal centrality).

ROI Analyses of Delayed Recall Memory

In all regions exhibiting CBF or GMV change after ECT, and in all hippocampal networks, post-hoc ROI analyses explored relationships between change in MRI metric and change in memory scores. A general linear model was used, where nuisance regressors included age, % depression score change, ECT electrode placement (% right-unilateral), and total number of treatments. No overall reductions in memory scores were noted after ECT, nor were interactions with antidepressant response present in this cohort (Supplemental Results) (27); therefore we targeted main effects of change in memory score for this analysis (i.e., rather than interactions with response). These analyses were considered exploratory and no correction for multiple comparisons was applied.

RESULTS

Demographic and clinical variables

Of volunteers who completed the post-ECT index study visit, 41% (18/44) were defined as responders, showing at least 50% average reduction in depression scores across the three inventories used (Table 1). Responders, nonresponders, and nondepressed controls did not differ in age or sex, and, as expected, nonresponders had on average ~2 more treatments and had a lesser proportion of right-unilateral ECT treatments than responders (73 vs 97% right-unilateral, respectively). Depression scores improved significantly in both groups after two treatments and after ECT index, which was maintained at 6 months.

Loci of hippocampal CBF change in responders and nonresponders to ECT

Separable loci of CBF change were identified that survived validation by subsampling (100% overlap at $p < 0.05$, $k > 25\text{mm}^3$; Figure 1&3, Table 2, Supplementary Table 1). In patients who responded to ECT, post-index CBF increases were identified in the right middle and left posterior hippocampus. In nonresponders, CBF increased in relatively larger

clusters located in the anterior hippocampi bilaterally, with effects more robust in the right hippocampus. These hippocampal clusters were retained as seed regions for subsequent analyses.

Loci of hippocampal GMV change in responders and nonresponders to ECT

In patients who did not respond to ECT, large bilateral increases in voxelwise GMV were noted after treatment. In responders, a small region of right anterior hippocampus overlapping the amygdala exhibited increased GMV after treatment (Figure 2&3, Table 2, Supplementary Table 2).

Hippocampal networks

Seed-based functional connectivity analyses of BOLD-fMRI data from non-depressed control volunteers established spatially separable functional networks associated with each hippocampal region identified in CBF analyses described above (Figure 4A). The anterior hippocampal seed defined a network similar to the default-mode network, and included the following regions: medial prefrontal cortex, posterior cingulate cortex, precuneus. The seed located in the middle of the hippocampus defined a network comprised of the basal ganglia and thalamus. Finally, the posterior hippocampal seed defined a network comprised of lateral and medial posterior parietal cortex, which is often designated as the posterior default mode network.

In graph theory analyses of these hippocampal networks (Figure 4B), a response-by-time interaction was identified in the hippocampus-thalamus-striatum network defined using the mid hippocampal seed (HCN-R1, Figure 4A), where network strength decreased after two treatments in ECT responders. This change persisted after index in responders, but did not change in nonresponders. Response-by-time interactions were not noted in connectivity metrics for the other two networks or hippocampal centrality (Supplementary Table 3, Supplementary Figure 1).

Correlations with recall memory

Post-ECT change in mean CBF in left anterior hippocampus was negatively correlated with post-ECT change in verbal recall, such that improved recall associated with decreased CBF ($p=0.02$). Relatedly, post-ECT change in anterior hippocampal network metrics (network strength and hippocampal centrality) were also negatively correlated with change in visuospatial scores, where improved performance associated with decreased connectivity.

Positive correlations were noted between GMV change after ECT and change in verbal recall. Here, increased GMV associated improved performance ($p<0.05$). Scatterplots for all correlations $p < 0.10$ are displayed in Figure 5 for this exploratory analysis (see also Supplemental Results and Supplementary Figure 2).

DISCUSSION

Hippocampal plasticity has long been associated with ECT, yet its relation to antidepressant outcome is not well understood. In our study, we identified structural and functional changes

in the hippocampi and surrounding regions associated with antidepressant response to ECT. Patients that did not respond to ECT exhibited increased CBF in bilateral anterior hippocampus, as well as robust increases in GMV bilaterally. In ECT responders, changes were more circumscribed, with CBF increases occurring in right middle and left posterior hippocampus, and GMV increases occurring in right anterior hippocampus. Notably, loci of CBF change were associated with separable functional networks, suggesting that plasticity in different hippocampal subregions could have downstream effects in different brain regions and networks. Indeed, graph theory analyses of these networks showed acute and post-index modulation of a hippocampus-thalamus-striatum network in ECT responders. Taken together, these results appear to indicate that the location of hippocampal plasticity may differ according to antidepressant response to ECT, and that excessive plasticity within the hippocampus and surrounding tissue may not associate with positive ECT outcome.

Hippocampal plasticity in ECT

A growing body of human and animal research associates ECT-induced seizures with many different forms of hippocampal plasticity. Markers of neurogenesis, synaptogenesis, gliogenesis, and other markers of cellular plasticity increase in animal models of ECT (6–8). In human neuroimaging studies, total hippocampal volume has been shown to increase after ECT in many studies (1–5, 13–15). Studies also demonstrate increases isolated to the dentate gyrus in high-field anatomical MRI (32, 33) and to right anterior hippocampus in surface-based morphometric analyses targeting primarily right-unilateral ECT (1). The current analyses reported here corroborate these neuroanatomical effects, while also supporting more extensive increases throughout the hippocampus and surrounding tissue in nonresponders to ECT and more circumscribed changes overlapping right amygdala in responders (c.f. (34) and Supplemental Results). Clearly, ECT very likely induces structural plasticity within the hippocampus and surrounding tissue, yet how these changes relate to neuroplasticity supporting antidepressant response remains unclear.

In our current study, neurofunctional changes appeared to occur in different subregions of the hippocampus along its anterior-posterior axis in responders and nonresponders to ECT as measured with ASL-fMRI. These different subregions were also linked with different functional brain networks, as supported by previous research (18, 19). Further, the extent of neurofunctional change appeared to be greater in patients who did not respond to ECT, mirroring our anatomical findings. Taken together, these results may indicate that the precise location (and/or spatial extent) of hippocampal plasticity may correlate with which brain networks are modulated by ECT. Many interpretations of these effects are possible, which are not mutually exclusive. Differing locations of hippocampal plasticity may reflect individual differences in the susceptibility of tissue to seizure activity, individual neuroanatomical differences affecting electrical current flow through medial temporal lobe tissue, variable influence of other brain networks on hippocampal activity during ECT-induced seizures (e.g., during seizure termination), or other factors. Future studies linking the physiology of ECT-induced seizure activity to long-term neuroplastic changes are needed to address these hypotheses. Whether GMV change occurs in different hippocampal subregions in responders and nonresponders to ECT should also be confirmed in studies

with ultra-high spatial resolution, perhaps targeting subregional change along the anterior-posterior axis of the dentate gyrus.

Linking long-term plasticity with seizure physiology in ECT

Generalized seizure of adequate length is purported to be important for a “successful” ECT session, evidenced by highly coordinated seizure activity at all/most recording sites during multi-channel EEG and motor symptoms (35). Thus, the process of seizure generalization appears to be integral to positive outcome (36), though other stages (i.e., initiation, termination) likely play a role as well (37, 38). Notably, evidence from animal models (39, 40), patients with epilepsy (41), and ECT (42–44) demonstrate that neuronal activity measured during generalized seizures is not homogenous throughout the brain (45). This suggests that different brain regions and networks may be engaged during different seizure stages during ECT, and perhaps that the degree to which these regions are efficiently engaged at each seizure stage may affect treatment outcome; yet, precise measurement of brain activity during different seizure stages during ECT is challenging and thus evidence is sparse.

SPECT studies have injected tracers before treatment to “tag” brain activity during different stages of ECT-induced seizures. These studies have shown increased activity in anteromedial temporal regions at the beginning of the ECT session, which is often interpreted as reflecting seizure initiation (46). After seizure initiation, however, brain-activity changes occur elsewhere during ECT-induced seizures, typically including increased thalamic and brainstem activity coupled with decreased cortical activity (46–49). The thalamus has been linked to the propagation of generalized seizures in animal models (50, 51), and the thalamus and/or thalamo-cortical networks are thought to play an important role in the generalization of seizures during ECT (46, 52).

In the current study, patients who responded to ECT exhibited increased CBF in a region of right middle hippocampus, which was functionally connected with a hippocampus-thalamus-striatum network. Notably, ECT responders showed acute and long-term changes in this network, exhibiting decreased network connectivity strength after two treatments and after completing treatment index. In our previous work in this cohort, we have also noted decreased pre-treatment thalamic CBF in responders that “normalized” after ECT (16), as well as modulation of thalamus-striatum-frontal functional connectivity after ECT related to antidepressant response (53). Taken together, these results suggest that the lasting neuroplastic effects of seizure generalization (and/or the transition from seizure initiation to generalization) may play a role in successful clinical outcome in ECT, perhaps in the form of long-term plasticity within thalamic networks.

Hippocampal plasticity and memory in ECT

Episodic memory, including autobiographical memories, may be affected in some patients undergoing ECT (54, 55). In our study, patients received predominantly right-unilateral ultra-brief-pulse ECT, explicitly chosen to reduce potential impairments in episodic autobiographical memory (54, 55). This may explain, at least in part, why this cohort did not appear to exhibit memory impairments after ECT. However, we did not assess episodic

autobiographical memory directly, and care must be taken when using experimental memory tasks to assess episodic memory impairments sometimes associated with this ECT. In our study, increased hippocampal volume after ECT correlated with improved delayed recall of words after treatment, suggesting that increased overall hippocampal GMV may not associate with memory-related side effects in ECT, in contrast to a recent report (56). Delayed recall of visuo-spatial items in our study was also modestly associated with changes in anterior hippocampus and its associated network, which has been linked with autobiographical memory in many previous neuroimaging studies (57). Interactions with antidepressant response were not apparent, either of the memory scores themselves, or of their relationships with brain markers. Future studies should assess whether these changes are associated with impaired episodic and/or autobiographical memory following ECT, an underrepresented topic in this field (27, 58).

Limitations and Conclusions

Several limitations should be considered. Primarily, independent validation of these results in a larger sample is needed, using ultra-high-resolution MRI data better able to resolve subfields/subnuclei of medial temporal lobe structures. ECT electrode placement was also not balanced in this naturalistic study, though the great majority received predominantly or only RUL ECT. Indeed, a recent mega-analysis showed that ECT electrode placement (bilateral versus RUL) affected the extent of volume change in left, but not right hippocampus (15). Multi-site studies like these will be better powered to address whether the laterality of hippocampal neuroplasticity is related to ECT electrode placement, pathophysiology underlying depression (59), or a combination of both. Such studies are also needed to parse the potential contributions of co-morbidities, ECT stimulation parameters, cognitive outcomes (27, 54), psychotropic medication history, and other factors on ECT-induced neuroplasticity. Our results suggest that patterns of functional and structural changes in the hippocampus after ECT may differ according to antidepressant response. In particular, the spatial location and extent of CBF change appears to differ in responders and nonresponders to ECT, which may associate with different patterns of down-stream plasticity in different hippocampal networks. Thus, although the distribution of electrical current applied at each electrode may be comparable during ECT (60, 61) and all patients experience generalized seizures (35), the regional distribution of ECT-induced seizure activity and/or its lasting functional effects may differ according to antidepressant response.

Supplementary Material

Refer to Web version on PubMed Central for supplementary material.

ACKNOWLEDGEMENTS

This work was supported by the NIH, including R01 MH092301 and U01 MH110008 to Drs. Narr and Espinoza and K24 MH102743 to Dr. Narr, the Muriel Harris Chair in Geriatric Psychiatry to Dr. Espinoza, as well as the Brian and Behavior Research Foundation, a NARSAD Young Investigator award to Dr. Leaver.

REFERENCES

1. Joshi SH, Espinoza RT, Pirnia T, Shi J, Wang Y, Ayers B, et al. (2015): Structural plasticity of the hippocampus and amygdala induced by electroconvulsive therapy in major depression. *Biol Psychiatry*. 79: 282–92. [PubMed: 25842202]
2. Tendolkar I, Beek M, Oostrom I, Mulder M, Janzing J, Voshaar RO, Eijndhoven P (2013): Electroconvulsive therapy increases hippocampal and amygdala volume in therapy refractory depression: a longitudinal pilot study. *Psychiatry Res*. 214: 197–203. [PubMed: 24090511]
3. Redlich R, Opel N, Grotegerd D, Dohm K, Zaremba D, Bürger C, et al. (2016): Prediction of Individual Response to Electroconvulsive Therapy via Machine Learning on Structural Magnetic Resonance Imaging Data. *JAMA Psychiatry*. 73: 557. [PubMed: 27145449]
4. Dukart J, Regen F, Kherif F, Colla M, Bajbouj M, Heuser I, et al. (2014): Electroconvulsive therapy-induced brain plasticity determines therapeutic outcome in mood disorders. *Proc Natl Acad Sci U S A*. 111: 1156–61. [PubMed: 24379394]
5. Cano M, Martínez-Zalacaín I, Bernabéu-Sanz Á, Contreras-Rodríguez O, Hernández-Ribas R, Via E, et al. (2017): Brain volumetric and metabolic correlates of electroconvulsive therapy for treatment-resistant depression: a longitudinal neuroimaging study. *Transl Psychiatry*. 7: e1023. [PubMed: 28170003]
6. Chen F, Madsen TM, Wegener G, Nyengaard JR (2009): Repeated electroconvulsive seizures increase the total number of synapses in adult male rat hippocampus. *Eur Neuropsychopharmacol*. 19: 329–338. [PubMed: 19176277]
7. Madsen TM, Treschow A, Bengzon J, Bolwig TG, Lindvall O, Tingström A (2000): Increased neurogenesis in a model of electroconvulsive therapy. *Biol Psychiatry*. 47: 1043–1049. [PubMed: 10862803]
8. Perera TD, Coplan JD, Lisanby SH, Lipira CM, Arif M, Carpio C, et al. (2007): Antidepressant-induced neurogenesis in the hippocampus of adult nonhuman primates. *J Neurosci Off J Soc Neurosci*. 27: 4894–4901.
9. Abbott CC, Jones T, Lemke NT, Gallegos P, McClintock SM, Mayer AR, et al. (2014): Hippocampal structural and functional changes associated with electroconvulsive therapy response. *Transl Psychiatry*. 4: e483. [PubMed: 25405780]
10. Leaver AM, Espinoza R, Pirnia T, Joshi SH, Woods RP, Narr KL (2016): Modulation of Intrinsic Brain Activity by Electroconvulsive Therapy in Major Depression. *Biol Psychiatry Cogn Neurosci Neuroimaging*. 1: 77–86. [PubMed: 26878070]
11. Argyelan M, Lencz T, Kaliora S, Sarpal DK, Weissman N, Kingsley PB, et al. (2016): Subgenual cingulate cortical activity predicts the efficacy of electroconvulsive therapy. *Transl Psychiatry*. 6: e789. [PubMed: 27115120]
12. Njau S, Joshi SH, Leaver AM, Vasavada M, Fleet J, Espinoza R, Narr KL (2016): Variations in myo-inositol in fronto-limbic regions and clinical response to electroconvulsive therapy in major depression. *J Psychiatr Res*. 80: 45–51. [PubMed: 27285661]
13. Takamiya A, Chung JK, Liang K, Graff-Guerrero A, Mimura M, Kishimoto T (2018): Effect of electroconvulsive therapy on hippocampal and amygdala volumes: systematic review and meta-analysis. *Br J Psychiatry*. 212: 19–26. [PubMed: 29433612]
14. Wilkinson ST, Sanacora G, Bloch MH (2017): Hippocampal Volume Changes Following Electroconvulsive Therapy: A Systematic Review and Meta-analysis. *Biol Psychiatry Cogn Neurosci Neuroimaging*. 2: 327–335. [PubMed: 28989984]
15. Olteidal L, Narr KL, Abbott C, Anand A, Argyelan M, Bartsch H, et al. (2018): Volume of the Human Hippocampus and Clinical Response Following Electroconvulsive Therapy. *Biol Psychiatry*. 84: 574–581. [PubMed: 30006199]
16. Leaver AM, Vasavada M, Joshi SH, Wade B, Woods RP, Espinoza R, Narr KL (2019): Mechanisms of Antidepressant Response to Electroconvulsive Therapy Studied With Perfusion Magnetic Resonance Imaging. *Biol Psychiatry*. 85: 466–476. [PubMed: 30424864]
17. Kubicki A, Leaver AM, Vasavada M, Njau S, Wade B, Joshi SH, et al. (2019): Variations in Hippocampal White Matter Diffusivity Differentiate Response to Electroconvulsive Therapy in

Major Depression. *Biol Psychiatry Cogn Neurosci Neuroimaging*. 4: 300–309. [PubMed: 30658916]

18. Strange BA, Witter MP, Lein ES, Moser EI (2014): Functional organization of the hippocampal longitudinal axis. *Nat Rev Neurosci*. 15: 655–669. [PubMed: 25234264]
19. Poppenk J, Evensmoen HR, Moscovitch M, Nadel L (2013): Long-axis specialization of the human hippocampus. *Trends Cogn Sci*. 17: 230–240. [PubMed: 23597720]
20. Joshi SH, Espinoza RT, Pirnia T, Shi J, Wang Y, Ayers B, et al. (2015): Structural plasticity of the hippocampus and amygdala induced by electroconvulsive therapy in major depression. *Biol Psychiatry*. 79: 282–92. [PubMed: 25842202]
21. Wade BSC, Joshi SH, Njau S, Leaver AM, Vasavada M, Woods RP, et al. (2016): Effect of Electroconvulsive Therapy on Striatal Morphometry in Major Depressive Disorder. *Neuropsychopharmacology*. 41: 2481–2491. [PubMed: 27067127]
22. Lyden H, Espinoza RT, Pirnia T, Clark K, Joshi SH, Leaver AM, et al. (2014): Electroconvulsive therapy mediates neuroplasticity of white matter microstructure in major depression. *Transl Psychiatry*. 4: e380. [PubMed: 24713861]
23. Pirnia T, Joshi SH, Leaver AM, Vasavada M, Njau S, Woods RP, et al. (2016): Electroconvulsive therapy and structural neuroplasticity in neocortical, limbic and paralimbic cortex. *Transl Psychiatry*. 6: e832. [PubMed: 27271858]
24. Leaver AM, Wade B, Vasavada M, Hellemann G, Joshi SH, Espinoza R, Narr KL (2018): Fronto-Temporal Connectivity Predicts ECT Outcome in Major Depression. *Front Psychiatry*. 9. doi: 10.3389/fpsyt.2018.00092.
25. Leaver AM, Espinoza R, Joshi SH, Vasavada M, Njau S, Woods RP, Narr KL (2016): Desynchronization and Plasticity of Striato-frontal Connectivity in Major Depressive Disorder. *Cereb Cortex N Y N 1991* 26: 4337–4346.
26. Njau S, Joshi SH, Espinoza R, Leaver AM, Vasavada M, Marquina A, et al. (2017): Neurochemical correlates of rapid treatment response to electroconvulsive therapy in patients with major depression. *J Psychiatry Neurosci JPN*. 42: 6–16. [PubMed: 27327561]
27. Vasavada MM, Leaver AM, Njau S, Joshi SH, Ercoli L, Hellemann G, et al. (2017): Short- and Long-term Cognitive Outcomes in Patients With Major Depression Treated With Electroconvulsive Therapy. *J ECT*. 33: 278–285. [PubMed: 28617690]
28. Bonner-Jackson A, Mahmoud S, Miller J, Banks SJ (2015): Verbal and non-verbal memory and hippocampal volumes in a memory clinic population. *Alzheimers Res Ther*. 7. doi: 10.1186/s13195-015-0147-9.
29. Gelbard-Sagiv H, Mukamel R, Harel M, Malach R, Fried I (2008): Internally Generated Reactivation of Single Neurons in Human Hippocampus During Free Recall. *Science*. 322: 96–101. [PubMed: 18772395]
30. Wang Z, Aguirre GK, Rao H, Wang J, Fernández-Seara MA, Childress AR, Detre JA (2008): Empirical optimization of ASL data analysis using an ASL data processing toolbox: ASLtbx. *Magn Reson Imaging*. 26: 261–269. [PubMed: 17826940]
31. Ashburner J, Friston KJ (2000): Voxel-Based Morphometry—The Methods. *NeuroImage*. 11: 805–821. [PubMed: 10860804]
32. Nuninga JO, Mandl RCW, Boks MP, Bakker S, Somers M, Heringa SM, et al. (2019): Volume increase in the dentate gyrus after electroconvulsive therapy in depressed patients as measured with 7T. *Mol Psychiatry*. doi: 10.1038/s41380-019-0392-6.
33. Takamiya A, Plitman E, Chung JK, Chakravarty M, Graff-Guerrero A, Mimura M, Kishimoto T (2019): Acute and long-term effects of electroconvulsive therapy on human dentate gyrus. *Neuropsychopharmacology*. doi: 10.1038/s41386-019-0312-0.
34. Redlich R, Bürger C, Dohm K, Grotegerd D, Opel N, Zaremba D, et al. (2017): Effects of electroconvulsive therapy on amygdala function in major depression - a longitudinal functional magnetic resonance imaging study. *Psychol Med*. 47: 2166–2176. [PubMed: 28397635]
35. Kellner CH, Pritchett JT, Beale MD, Coffey CE (1997): *Handbook of ECT*. Washington, D.C.: American Psychiatric Press.
36. Jan Shah A, Wadoo O, Latoo J (2013): Electroconvulsive Therapy (ECT): Important parameters which influence its effectiveness. *Br J Med Pract*. 6: 31–36.

37. Kayser S, Bewernick BH, Soehle M, Switala C, Gippert SM, Dreimueller N, Schlaepfer TE (2017): Degree of Postictal Suppression Depends on Seizure Induction Time in Magnetic Seizure Therapy and Electroconvulsive Therapy. *J ECT*. 33: 167–175. [PubMed: 28640168]
38. Perera TD, Lubner B, Nobler MS, Prudic J, Anderson C, Sackeim HA (2004): Seizure expression during electroconvulsive therapy: relationships with clinical outcome and cognitive side effects. *Neuropsychopharmacol Off Publ Am Coll Neuropsychopharmacol*. 29: 813–825.
39. Nersesyan H, Hyder F, Rothman DL, Blumenfeld H (2004): Dynamic fMRI and EEG recordings during spike-wave seizures and generalized tonic-clonic seizures in WAG/Rij rats. *J Cereb Blood Flow Metab*. 24: 589–599. [PubMed: 15181366]
40. Blumenfeld H, McCormick DA (2000): Corticothalamic Inputs Control the Pattern of Activity Generated in Thalamocortical Networks. *J Neurosci*. 20: 5153–5162. [PubMed: 10864972]
41. Blumenfeld H, Varghese GI, Purcaro MJ, Motelow JE, Enev M, McNally KA, et al. (2009): Cortical and subcortical networks in human secondarily generalized tonic-clonic seizures. *Brain J Neurol*. 132: 999–1012.
42. Miller JW (2010): Are Generalized Tonic–Clonic Seizures Really “Generalized”? *Epilepsy Curr*. 10: 80–81. [PubMed: 20697499]
43. Enev M, McNally KA, Varghese G, Zupal IG, Ostroff RB, Blumenfeld H (2007): Imaging onset and propagation of ECT-induced seizures. *Epilepsia*. 48: 238–44. [PubMed: 17295616]
44. Blumenfeld H, Westerveld M, Ostroff RB, Vanderhill SD, Freeman J, Necochea A, et al. (2003): Selective frontal, parietal, and temporal networks in generalized seizures. *NeuroImage*. 19: 1556–1566. [PubMed: 12948711]
45. McNally KA, Blumenfeld H (2004): Focal network involvement in generalized seizures: new insights from electroconvulsive therapy. *Epilepsy Behav*. 5: 3–12. [PubMed: 14751200]
46. Enev M, McNally KA, Varghese G, Zupal IG, Ostroff RB, Blumenfeld H (2007): Imaging onset and propagation of ECT-induced seizures. *Epilepsia*. 48: 238–244. [PubMed: 17295616]
47. Blumenfeld H, Varghese GI, Purcaro MJ, Motelow JE, Enev M, McNally KA, et al. (2009): Cortical and subcortical networks in human secondarily generalized tonic–clonic seizures. *Brain*. 132: 999–1012. [PubMed: 19339252]
48. Takano H, Motohashi N, Uema T, Ogawa K, Ohnishi T, Nishikawa M, Matsuda H (2011): Differences in cerebral blood flow between missed and generalized seizures with electroconvulsive therapy: A positron emission tomographic study. *Epilepsy Res*. 97: 225–228. [PubMed: 21917425]
49. Takano H, Motohashi N, Uema T, Ogawa K, Ohnishi T, Nishikawa M, et al. (2007): Changes in regional cerebral blood flow during acute electroconvulsive therapy in patients with depression: Positron emission tomographic study. *Br J Psychiatry*. 190: 63–68. [PubMed: 17197658]
50. McCormick DA, Contreras D (2001): On The Cellular and Network Bases of Epileptic Seizures. *Annu Rev Physiol*. 63: 815–846. [PubMed: 11181977]
51. Bertram EH, Zhang D, Williamson JM (2008): Multiple roles of midline dorsal thalamic nuclei in induction and spread of limbic seizures. *Epilepsia*. 49: 256–268. [PubMed: 18028408]
52. Bolwig TG (2011): How does electroconvulsive therapy work? Theories on its mechanism. *Can J Psychiatry Rev Can Psychiatr*. 56: 13–18.
53. Leaver AM, Espinoza R, Pirnia T, Joshi SH, Woods RP, Narr KL (2016): Modulation of Intrinsic Brain Activity by Electroconvulsive Therapy in Major Depression. *Biol Psychiatry Cogn Neurosci Neuroimaging*. 1: 77–86. [PubMed: 26878070]
54. Lisanby SH, Maddox JH, Prudic J, Devanand DP, Sackeim HA (2000): The Effects of Electroconvulsive Therapy on Memory of Autobiographical and Public Events. *Arch Gen Psychiatry*. 57: 581–590. [PubMed: 10839336]
55. Kessler U, Schoeyen HK, Andreassen OA, Eide GE, Malt UF, Oedegaard KJ, et al. (2014): The effect of electroconvulsive therapy on neurocognitive function in treatment-resistant bipolar disorder depression. *J Clin Psychiatry*. 75: e1306–1313. [PubMed: 25470096]
56. van Oostrom I, van Eijndhoven P, Butterbrod E, van Beek MH, Janzing J, Donders R, et al. (2018): Decreased Cognitive Functioning After Electroconvulsive Therapy Is Related to Increased Hippocampal Volume: Exploring the Role of Brain Plasticity. *J ECT*. 34: 117–123. [PubMed: 29389676]

57. Zeidman P, Maguire EA (2016): Anterior hippocampus: the anatomy of perception, imagination and episodic memory. *Nat Rev Neurosci.* 17: 173–182. [PubMed: 26865022]
58. Szabo K, Hirsch JG, Krause M, Ende G, Henn FA, Sartorius A, Gass A (2007): Diffusion weighted MRI in the early phase after electroconvulsive therapy. *Neurol Res.* 29: 256–259. [PubMed: 17509223]
59. Sheline YI, Sanghavi M, Mintun MA, Gado MH (1999): Depression Duration But Not Age Predicts Hippocampal Volume Loss in Medically Healthy Women with Recurrent Major Depression. *J Neurosci.* 19: 5034–5043. [PubMed: 10366636]
60. Bai S, Loo C, Al Abed A, Dokos S (2012): A computational model of direct brain excitation induced by electroconvulsive therapy: comparison among three conventional electrode placements. *Brain Stimulat.* 5: 408–421.
61. Lee WH, Deng Z-D, Kim T-S, Laine AF, Lisanby SH, Peterchev AV (2012): Regional electric field induced by electroconvulsive therapy in a realistic finite element head model: Influence of white matter anisotropic conductivity. *NeuroImage.* 59: 2110–2123. [PubMed: 22032945]

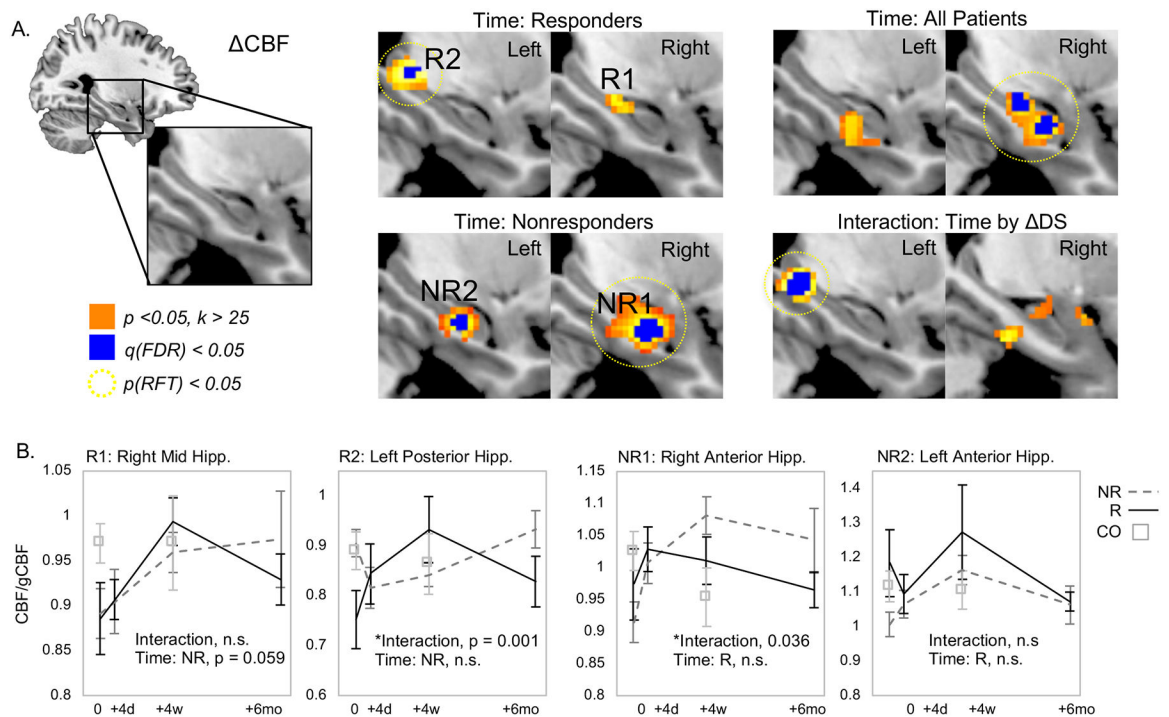


Figure 1.

Regional CBF increases in responders and nonresponders to ECT within the hippocampus and surrounding tissue. **A.** Resting brain function measured with CBF increased over time (pre-treatment vs. post-index) in right middle and left posterior hippocampus in patients who responded to ECT (top left), while CBF increased in bilateral anterior hippocampus after ECT in responders (bottom left). Regions of increased CBF in all patients (top right) and interaction between time and response (bottom right) are also displayed. **B.** Mean regional CBF (corrected for global CBF) is plotted for the significant results shown in A for clusters of CBF change in responders and nonresponders. In each plot, data for responders is shown in black lines, nonresponders are plotted in dashed gray lines, and data from non-depressed control volunteers is plotted in open squares.

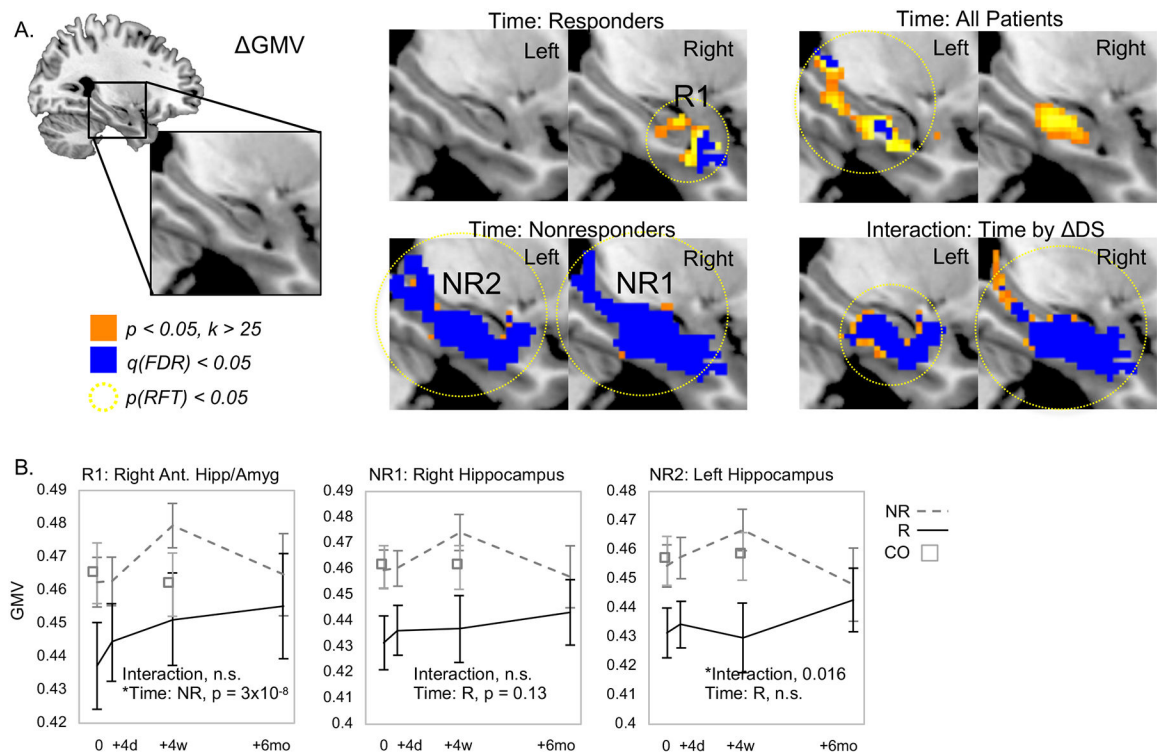
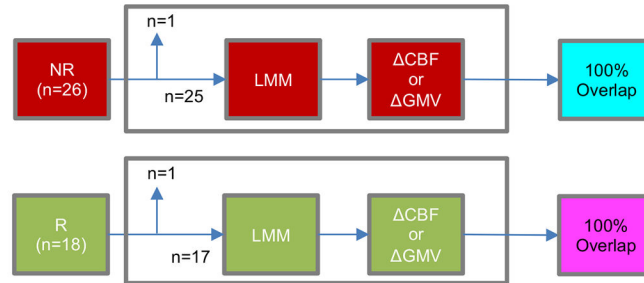
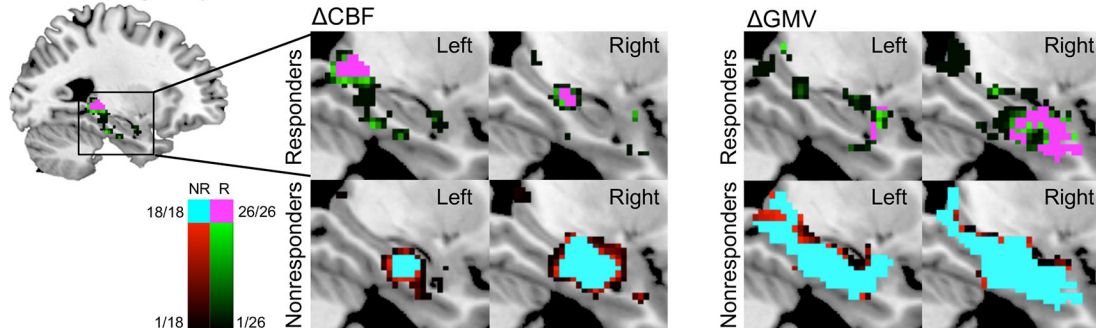


Figure 2. Regional GMV increases after ECT in responders and nonresponders. **A.** GMV increased in right anterior hippocampus and amygdala in responders (top left) and throughout bilateral hippocampus in nonresponders after ECT (bottom left). Regions of increased GMV when analyzing all patients (upper right) and interactions between time and response (bottom right) area also displayed. **B.** Mean regional GMV is plotted for the significant results shown in A for clusters of GMV change identified in responders and for nonresponders. In each plot, data for responders is shown in black lines, nonresponders are plotted in dashed gray lines, and data from non-depressed control volunteers is plotted in open squares.

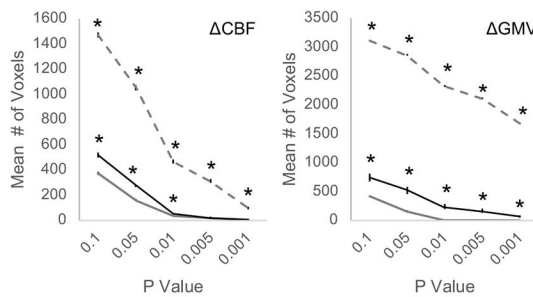
A. Subsampling Schematic



B. Subsampling Analyses



C. Mean Voxel Count



D. Max Cluster Size

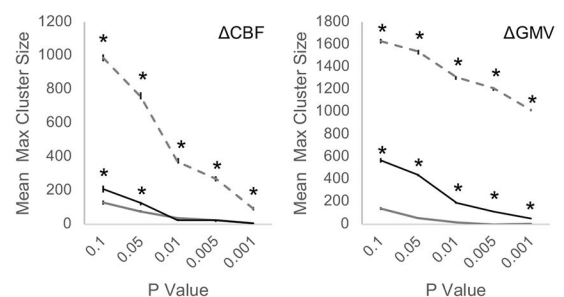
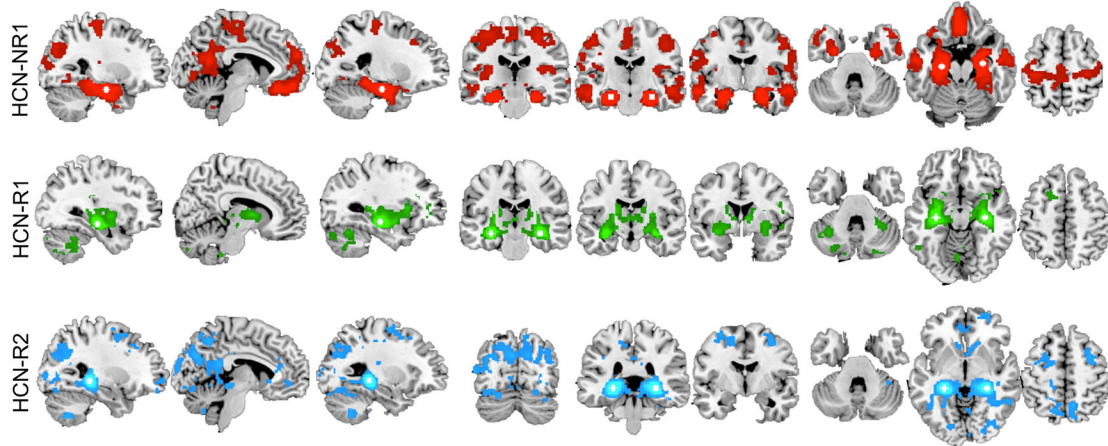


Figure 3.

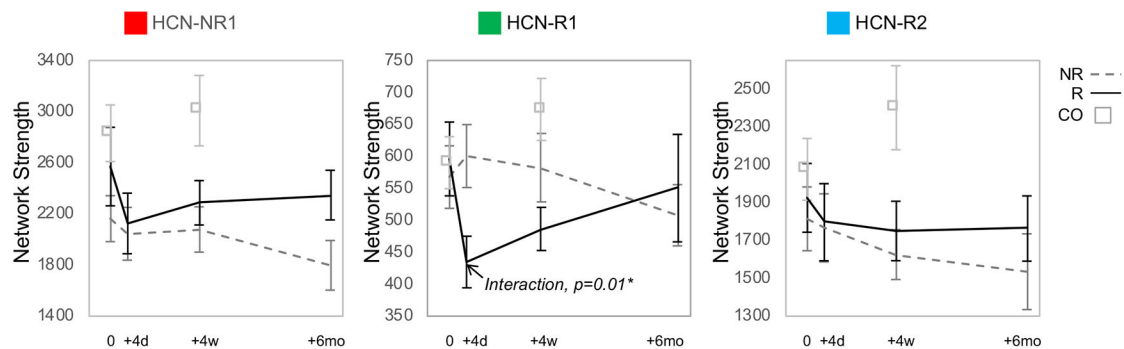
Leave-one-out (LOO) subsampling validates the location of CBF and GMV increases in responders (R) and nonresponders (NR) to ECT. **A.** A schematic illustrates the validation method applied. For each group, data from one volunteer was removed from the dataset, and a linear mixed effects model (LMM) was applied to the remaining subsample to identify maps of significant change () in CBF and (separately) GMV after ECT, voxelwise $p < 0.05$. This process was applied iteratively across all possible subsamples, and maps of 100% overlap across all subsamples were generated. Clusters $k > 25$ of voxels exhibiting 100% subsample overlap were considered significant, and retained for follow-up analysis with BOLD-fMRI data (for CBF clusters). **B.** Overlap maps are displayed for CBF (left panels) and GMV (right panels), separately validated in responders (top panels) and nonresponders (bottom panels). Voxel color denotes overlap across subsamples at $p < 0.05$ for responders in green and nonresponders in red; regions of 100% overlap $k > 25$ are shown in pink for responders and cyan for nonresponders. Note the locations of 100% overlap match clusters shown in Figures 1 & 2. **C&D.** The choice of voxelwise threshold $p < 0.05$ was exploratory

and arguably arbitrary; therefore, mean voxel counts (**C**) and max cluster size (**D**) for across LOO subsamples are displayed for several voxelwise thresholds (x-axes). Asterisks mark values significantly higher than those obtained from control data (FDR-corrected $p < 0.05$; Supplemental Results).

A. Hippocampal Functional Networks (HCNs)



B. Post-ECT Changes in Hippocampal Functional Networks (HCNs)

**Figure 4.**

Seed-based functional connectivity analyses of BOLD-fMRI data from non-depressed control volunteers established spatially separable functional networks associated with each hippocampal region exhibiting regional CBF change validated with LOO subsampling (Figure 3). **A.** The hippocampal functional network (HCN) associated with regions of CBF change identified in nonresponders (NR) is shown in red (HCN-NR1), the network associated with increased CBF in right mid hippocampus in responders (R) is shown in green (HCN-R1), and in left posterior hippocampus in blue (HCN-R2). The location of the pair of seed regions used to define each network is displayed in white. **B.** Graph theory analyses assessed changes in network strength and hippocampal centrality over treatment course. Plots of network strength over time are displayed, with data from responders plotted in a solid black line, and data from nonresponders plotted in a dashed gray line. Corresponding hippocampal centrality data can be found in Supplementary Figure 1.

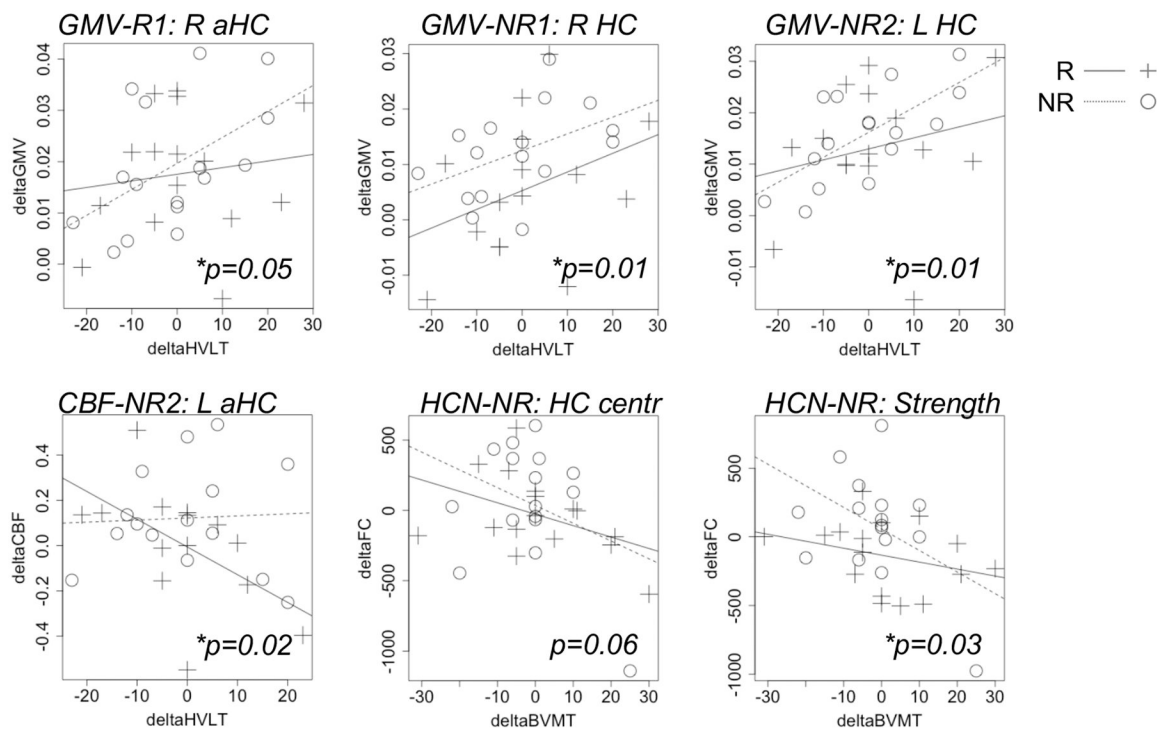


Figure 5. Post-treatment changes (delta) in MRI metrics were modestly correlated with changes in memory scores in some hippocampal subregions and networks. Scatter plots display relationships between recall scores and hippocampal metrics $p < 0.10$ for this exploratory analysis.

Table 1.

Demographic and Clinical Information

	Responders	Nonresponders	Controls
Sample Size	n = 18	n = 26	n = 36
Age, mean (SD)	43.53 (13.17)	39.50 (13.97)	39.06 (12.29)
Sex, females/males	7/10	16/10	19/17
Clinical Information			
Diagnosis, unipolar/bipolar	13/4	21/5	
Age at 1st diagnosed depressive episode, mean (SD)	27.24 (12.31)	23.12 (12.14)	
ECT electrode placement, only-RUL/other	15/2	11/15 ^a	
Number of ECT Index Treatments	10.35 (2.62)	12.62 (3.57) ^a	
Baseline Study Visit			
HAM-17, mean (SD)	27.06 (5.60)	22.27 (4.98) ^a	
MADRS, mean (SD)	43.71 (7.40)	33.69 (5.73) ^a	
QIDS-SR, mean (SD)	21.71 (3.51)	18.73 (3.99) ^a	
Corrected Sample Size, ASL/Other	18/18	26/26	32/32
Post-2tx Study Visit			
HAM-17, mean (SD)	19.88 (6.20) ^{b,c}	16.5 (7.55) ^{a,b,c}	
MADRS, mean (SD)	32.76 (7.78) ^{b,c}	25.20 (11.83) ^{b,c}	
QIDS-SR, mean (SD)	16.35 (4.65) ^{b,c}	14.60 (6.67) ^{b,c}	
Corrected Sample Size, ASL/Other	17/18	26/26	n/a
Post-Index (4wk) Study Visit			
HAM-17, mean (SD)	7.12 (3.53) ^{b,c}	17.50 (6.23) ^{a,b,c}	
MADRS, mean (SD)	8.59 (5.30) ^{b,c}	26.35 (8.04) ^{a,b}	
QIDS-SR, mean (SD)	6.76 (4.02) ^{b,c}	14.23 (4.81) ^{a,b,c}	
Corrected Sample Size, ASL/Other	17/18	26/26	33/33
Post-6mo Study Visit			
HAM-17, mean (SD)	12.80 (8.23) ^{b,c}	10.71 (6.91) ^{b,c}	
MADRS, mean (SD)	18.20 (13.41) ^{b,c}	16.00 (11.70) ^{b,c}	
QIDS-SR, mean (SD)	11.13 (5.57) ^{b,c}	9.65 (6.11) ^{b,c}	
Corrected Sample Size, ASL/Other	14/15	18/18	n/a

Results of chi-squared and t-tests are indicated as follows:

^a Significant difference between Responders and Nonresponders, $p < 0.05$,

^b significant difference between baseline and follow-up (within group), $p < 0.005$,

^c Significant difference from previous visit (within group), $p < 0.02$. All other comparisons were not significant.

Table 2.

Locations of CBF & GMV Change after ECT

Statistical Model	Anatomical Description	MNI Coordinates (Center of Gravity)			Volume (mm ³)
		X	Y	Z	
CBF-R-Main	Right mid hippocampus	30.4	-20.2	-11.9	512
	Left posterior hippocampus	-25.9	-33.6	-2.0	1304
CBF-R-Validated	Right mid hippocampus	30.6	-20.3	-11.6	296
	Left posterior hippocampus	-26.5	-31.8	-1.7	488
CBF-NR-Main	Right ant hippocampus	26.3	-13.7	-19.8	5152
	Left ant hippocampus	-24.8	-17.0	-19.3	1896
CBF-NR-Validated	Right ant hippocampus	26.2	-12.9	-19.8	5094
	Left ant hippocampus	-24.7	-16.8	-19.4	1450
GMV-R-Main	Right ant hippocampus/amygdala	29.1	-5.92	-23.5	3443
GMV-R-Validated	Right ant hippocampus/amygdala	29.3	-5.75	-24.2	3192
GMV-NR-Main	Right hippocampus+	25.5	-14.4	-17.8	20436
	Left hippocampus+	-24.3	-19.7	-15.3	19264
GMV-NR-Validated	Right hippocampus+	26.0	-13.6	-19.0	21015
	Left hippocampus+	-24.8	-17.9	-17.2	17840
	Left hippocampus	-15.5	-34.7	-6.2	459

Notes. Cluster locations are given in MNI (Montreal Neurological Institute) coordinates for changes in cerebral blood flow (CBF) and gray matter volume (GMV) in responders (R) and nonresponders (NR) to ECT both in main statistical models (Main) and after leave-one-out subsampling validation (Validated).